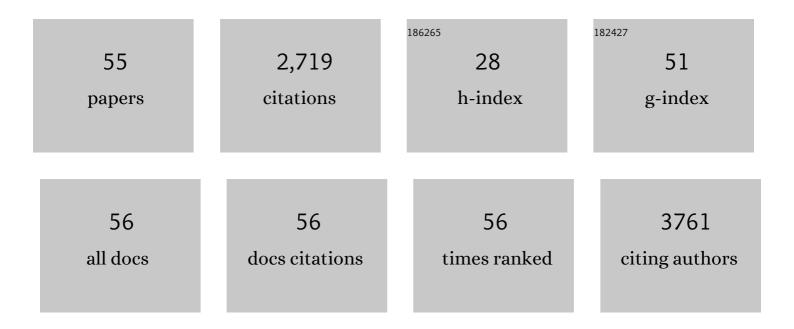


List of Publications by Year in descending order

Source: https://exaly.com/author-pdf/982369/publications.pdf Version: 2024-02-01



Ιινις Χιι

#	Article	IF	CITATIONS
1	In-situ growth of heterophase Ni nanocrystals on graphene for enhanced catalytic reduction of 4-nitrophenol. Nano Research, 2022, 15, 1230-1237.	10.4	21
2	Revealing the dependence of CO ₂ activation on hydrogen dissociation ability over supported nickel catalysts. AICHE Journal, 2022, 68, e17458.	3.6	9
3	Model-Based Analysis for Ethylene Carbonate Hydrogenation Operation in Industrial-Type Tubular Reactors. Processes, 2022, 10, 688.	2.8	1
4	Revealing synergetic structural activation of a CuAu surface during water–gas shift reaction. Proceedings of the National Academy of Sciences of the United States of America, 2022, 119, .	7.1	5
5	Unraveling the Role of Zinc on Bimetallic Fe ₅ C ₂ –ZnO Catalysts for Highly Selective Carbon Dioxide Hydrogenation to High Carbon α-Olefins. ACS Catalysis, 2021, 11, 2121-2133.	11.2	72
6	Revealing the Effect of Sodium on Iron-Based Catalysts for CO ₂ Hydrogenation: Insights from Calculation and Experiment. Journal of Physical Chemistry C, 2021, 125, 7637-7646.	3.1	20
7	Strong Metal–Support Interactions between Nickel and Iron Oxide during CO ₂ Hydrogenation. ACS Catalysis, 2021, 11, 11966-11972.	11.2	36
8	Effect of micropores on the structure and CO ₂ methanation performance of supported Ni/SiO ₂ catalyst. , 2021, 11, 1213-1221.		3
9	Ternary Fe–Zn–Al Spinel Catalyst for CO ₂ Hydrogenation to Linear α-Olefins: Synergy Effects between Al and Zn. ACS Sustainable Chemistry and Engineering, 2021, 9, 13818-13830.	6.7	20
10	Activation and deactivation of the commercialâ€ŧype CuO–Cr ₂ O ₃ –Fe ₂ O ₃ high temperature shift catalyst. AICHE Journal, 2020, 66, e16846.	3.6	14
11	Phase-controlled synthesis of Ni nanocrystals with high catalytic activity in 4-nitrophenol reduction. Journal of Materials Chemistry A, 2020, 8, 22143-22154.	10.3	22
12	Structure–Activity Relationship of the Polymerized Cobalt Phthalocyanines for Electrocatalytic Carbon Dioxide Reduction. Journal of Physical Chemistry C, 2020, 124, 16501-16507.	3.1	16
13	Essential Role of the Support for Nickel-Based CO ₂ Methanation Catalysts. ACS Catalysis, 2020, 10, 14581-14591.	11.2	165
14	Degradation of MO and H 2 O 2 on Cu/ γâ€Al 2 O 3 pellets in a fixed bed reactor: Kinetics and transport characteristics. AICHE Journal, 2020, 66, e17000.	3.6	9
15	Nature of Reactive Oxygen Intermediates on Copper-Promoted Iron–Chromium Oxide Catalysts during CO ₂ Activation. ACS Catalysis, 2020, 10, 7857-7863.	11.2	44
16	Effects of Cerium Doping on Pt–Sn/Al ₂ O ₃ Catalysts for <i>n</i> -Heptane Reforming. Industrial & Engineering Chemistry Research, 2020, 59, 6424-6434.	3.7	20
17	Unraveling Highly Tunable Selectivity in CO ₂ Hydrogenation over Bimetallic In-Zr Oxide Catalysts. ACS Catalysis, 2019, 9, 8785-8797.	11.2	139
18	Structureâ€Tunable Copper–Indium Catalysts for Highly Selective CO ₂ Electroreduction to CO or HCOOH. ChemSusChem, 2019, 12, 3955-3959.	6.8	55

Jing Xu

#	Article	IF	CITATIONS
19	Covalently Grafting Cobalt Porphyrin onto Carbon Nanotubes for Efficient CO ₂ Electroreduction. Angewandte Chemie, 2019, 131, 6667-6671.	2.0	26
20	Covalently Grafting Cobalt Porphyrin onto Carbon Nanotubes for Efficient CO ₂ Electroreduction. Angewandte Chemie - International Edition, 2019, 58, 6595-6599.	13.8	190
21	Strong Metal–Support Interactions between Copper and Iron Oxide during the Highâ€Temperature Waterâ€Gas Shift Reaction. Angewandte Chemie - International Edition, 2019, 58, 9083-9087.	13.8	82
22	Strong Metal–Support Interactions between Copper and Iron Oxide during the Highâ€Temperature Waterâ€Gas Shift Reaction. Angewandte Chemie, 2019, 131, 9181-9185.	2.0	22
23	Electronic Tuning of Cobalt Porphyrins Immobilized on Nitrogen-Doped Graphene for CO ₂ Reduction. ACS Applied Energy Materials, 2019, 2, 2435-2440.	5.1	34
24	Facile synthesis of polymerized cobalt phthalocyanines for highly efficient CO ₂ reduction. Green Chemistry, 2019, 21, 6056-6061.	9.0	33
25	Electrochemical Getters: A Novel Approach toward Improved Thermal Insulation. Journal of the Electrochemical Society, 2019, 166, B1701-B1706.	2.9	1
26	Cooperative Catalysis of Nickel and Nickel Oxide for Efficient Reduction of CO ₂ to CH ₄ . ChemCatChem, 2019, 11, 1295-1302.	3.7	25
27	Copper/carbon composites from waste printed circuit boards as catalysts for Fentonâ€like degradation of Acid Orange 7 enhanced by ultrasound. AICHE Journal, 2019, 65, 1234-1244.	3.6	16
28	Effects of the Facet Orientation of γâ€Al ₂ O ₃ Support on the Direct Synthesis of H ₂ O ₂ Catalyzed by Pd Nanoparticles. European Journal of Inorganic Chemistry, 2018, 2018, 1715-1725.	2.0	12
29	Operando Spectroscopic Study of Dynamic Structure of Iron Oxide Catalysts during CO ₂ Hydrogenation. ChemCatChem, 2018, 10, 1272-1276.	3.7	78
30	Hydrogenated Blue Titania for Efficient Solar to Chemical Conversions: Preparation, Characterization, and Reaction Mechanism of CO ₂ Reduction. ACS Catalysis, 2018, 8, 1009-1017.	11.2	223
31	Tuning the Dynamic Interfacial Structure of Copper–Ceria Catalysts by Indium Oxide during CO Oxidation. ACS Catalysis, 2018, 8, 5261-5275.	11.2	100
32	Fentonâ€like degradation of rhodamine B over highly durable Cuâ€embedded alumina: Kinetics and mechanism. AICHE Journal, 2018, 64, 538-549.	3.6	52
33	Structure Evolution of Co–CoO _{<i>x</i>} Interface for Higher Alcohol Synthesis from Syngas over Co/CeO ₂ Catalysts. ACS Catalysis, 2018, 8, 8606-8617.	11.2	90
34	MnO _x promotional effects on olefins synthesis directly from syngas over bimetallic Feâ€MnO _x /SiO ₂ catalysts. AICHE Journal, 2017, 63, 4451-4464.	3.6	34
35	Pulse Reverse Plating of Zn-Ni on Aluminum and Steel. ECS Transactions, 2017, 77, 1237-1245.	0.5	1
36	Effects of preparation methods on the activity of CuO/CeO2 catalysts for CO oxidation. Frontiers of Chemical Science and Engineering, 2017, 11, 603-612.	4.4	47

Jing Xu

#	Article	IF	CITATIONS
37	Direct and Selective Synthesis of Hydrogen Peroxide over Palladium–Tellurium Catalysts at Ambient Pressure. ChemSusChem, 2017, 10, 3342-3346.	6.8	57
38	Atmospheric, Non-Contact and High Speed Electro Chemical Machining Processes for X-ray Optics. ECS Transactions, 2017, 77, 1255-1270.	0.5	0
39	Synthesis and identification of hierarchical γ-AlOOH self-assembled by nanosheets with adjustable exposed facets. CrystEngComm, 2016, 18, 4546-4554.	2.6	18
40	Dispersing Pd nanoparticles on N-doped TiO ₂ : a highly selective catalyst for H ₂ O ₂ synthesis. Catalysis Science and Technology, 2016, 6, 5060-5068.	4.1	36
41	Degradation of trichloroethylene by hydrodechlorination using formic acid as hydrogen source over supported Pd catalysts. Journal of Hazardous Materials, 2016, 305, 178-189.	12.4	31
42	Quantitative In Situ Differential Reflectance Spectroscopy Analysis of Polycrystalline Platinum Oxidation in an Aqueous Acidic Electrolyte. ECS Electrochemistry Letters, 2015, 4, H46-H49.	1.9	1
43	Probing The Structure Evolution of Ironâ€Based Fischer–Tropsch to Produce Olefins by Operando Raman Spectroscopy. ChemCatChem, 2015, 7, 752-756.	3.7	40
44	The generation of hydroxyl radicals by hydrogen peroxide decomposition on <scp>F</scp> eOCl/SBAâ€15 catalysts for phenol degradation. AICHE Journal, 2015, 61, 166-176.	3.6	75
45	The Oxidation of Bromide on Platinum Electrodes in Aqueous Acidic Solutions: Electrochemical and In Situ Spectroscopic Studies. Journal of the Electrochemical Society, 2014, 161, H392-H398.	2.9	25
46	Kinetic study of higher alcohol synthesis directly from syngas over CoCu/SiO ₂ catalysts. AICHE Journal, 2014, 60, 1797-1809.	3.6	53
47	Quantitative Correlations between the Normal Incidence Differential Reflectance and the Coverage of Adsorbed Bromide on a Polycrystalline Platinum Rotating Disk Electrode. Analytical Chemistry, 2013, 85, 2795-2801.	6.5	9
48	Porous Teflon Ring-Solid Disk Electrode Arrangement for Differential Mass Spectrometry Measurements in the Presence of Convective Flow Generated by a Jet Impinging Electrode in the Wall-Jet Configuration. Analytical Chemistry, 2012, 84, 5175-5179.	6.5	7
49	Mechanistic insights into methanolâ€ŧoâ€olefin reaction on an αâ€Mn ₂ O ₃ nanocrystal catalyst. AICHE Journal, 2012, 58, 3474-3481.	3.6	5
50	Iron oxide and alumina nanocomposites applied to Fischer–Tropsch synthesis. Chemical Communications, 2011, 47, 4019.	4.1	44
51	Biphasic Pdâ^'Au Alloy Catalyst for Low-Temperature CO Oxidation. Journal of the American Chemical Society, 2010, 132, 10398-10406.	13.7	363
52	Hydroxyapatite Foam as a Catalyst for Formaldehyde Combustion at Room Temperature. Journal of the American Chemical Society, 2010, 132, 13172-13173.	13.7	110
53	Synthesis and Crystal Structure of an Unprecedented Supramolecular Complex [Co(µ ₂ â€ClO ₄) ₂ (H ₂ O) ₂]·2MA. Chinese Journal of Chemistry, 2009, 27, 501-504.	4.9	3
54	Synthesis, structure and property of cobalt(II) complexes with 3,5-di(1H-imidazol-1-yl)benzoic acid. CrystEngComm, 2009, 11, 873.	2.6	55

#	Article	IF	CITATIONS
55	Metal–organic frameworks with six- and four-fold interpenetration and their photoluminescence and adsorption property. CrystEngComm, 2009, 11, 2728.	2.6	50